SIGNATURES OF THE NIGHTSIDE OPEN-CLOSED MAGNETIC FIELD-LINE BOUNDARY DURING MODERATELY DISTURBED CONDITIONS AND IONOSPHERIC SUBSTORMS

M. L. Parkinson[1], M. Pinnock[2], P. L. Dyson[1], and J. C. Devlin[3]

[1]*Department of Physics, La Trobe University, Melbourne, Victoria 3086, Australia*
[2]*British Antarctic Survey, Natural Environment Research Council, Cambridge CB3 0ET, UK*
[3]*Department of Electronic Engineering, La Trobe University, Melbourne, Victoria 3086, Australia*

ABSTRACT

The comparatively low latitude of the Tasman International Geospace Environment Radar (TIGER) (147.2°E, 43.4°S, geographic; –54.6°Λ), a Southern Hemisphere HF SuperDARN radar, facilitates the observation of extensive backscatter from decametre-scale irregularities drifting in the auroral and polar cap ionosphere in the midnight sector. The radar often detects a persistent, sharp increase over ~90 km of range in line-of-sight Doppler velocity spread, or spectral width, from <50 m s^{-1} at lower latitude to >200 m s^{-1} at higher latitude. It was previously shown that for moderately disturbed conditions in the pre-midnight sector, the location of the spectral width boundary (SWB) corresponds to the poleward edge of the auroral oval determined using energy spectra of precipitating particles measured on board Defense Meteorology Satellite Program satellites. This implies the radar SWB is a proxy for the open-closed magnetic field-line boundary (OCB) under these particular conditions. Here we investigate whether the radar SWB is aligned with the satellite OCB under a broader range of geomagnetic conditions including small to moderate substorms occurring in the pre- and post-magnetic midnight sectors.

INTRODUCTION

The Super Dual Auroral Radar Network (SuperDARN) presently consists of 15 HF backscatter radars, each with a similar design optimised to measure ionospheric convection on a global scale (Greenwald et al. 1995). The radars employ phased antenna arrays to sequentially step the main beam through 16 directions separated in azimuth by 3.24° to form 52°-wide scans. Each radar attempts to record echo parameters, including the backscatter power, line-of-sight Doppler velocity, and Doppler velocity spread (or "spectral width"), once every 1–2 minutes at any of the 75 ranges between 180 to 3555 km in 45-km steps. The spectral widths are a measure of space and time variations in the line-of-sight velocity occurring within the sampling volume and integration time.

A sharp increase in the spectral widths from <50 m s^{-1} at lower latitude to >200 m s^{-1} at higher latitude is often observed in the dayside ionosphere, and has been interpreted as a proxy for the open-closed magnetic field line boundary (OCB) when the interplanetary magnetic field (IMF) B_z component is southward (Baker et al. 1995). A similar spectral width boundary (SWB) is sometimes observed in the nightside ionosphere, and it seems natural to consider whether it may also correspond to the OCB. The case studies to date have suggested the nightside SWB corresponds to the boundary between the central plasma sheet (CPS) and the so-called boundary plasma sheet (BPS) (Dudeney at al. 1998), the OCB (Lester et al. 2001; Parkinson et al. 2002), and other unidentified boundaries, depending on the prevailing geophysical and HF propagation conditions.

The purpose of this paper is to further investigate the relationship of the nightside SWB to magnetospheric boundaries under a broad range of geophysical conditions. For example, does the alignment of the SWB with the OCB change with MLT and geomagnetic activity? Does the SWB agree with the OCB during ionospheric substorms? Down to what spatial and temporal scales is the SWB an accurate proxy for the OCB? These are

important questions to address because using SuperDARN observations to specify the location and shape of magnetospheric boundaries is a potentially valuable contribution to the wider space science effort.

EXPERIMENT

Because the Tasman International Geospace Environment Radar (TIGER) is one of the most equatorward of the SuperDARN radars (–54.6°Λ), it routinely detects the SWB in the midnight sector during moderately disturbed conditions and substorms. Here we analyse observations made during the two representative nights of September 5 and October 31, 2000. Range-time plots of spectral widths for the magnetic meridian pointing beam 4 are shown because full-scan observations confirm the midnight SWB is roughly aligned in a zonal direction, and thus will be sharper and more accurately located using an orthogonal beam. The SWB was automatically identified as the poleward edge of the most equatorward range cell with spectral width <200 m s^{-1}, whilst the next two range cells had a spectral width ≥200 m s^{-1}, and the subsequent two range cells had spectral widths ≥100 m s^{-1}. These conditions ensured the SWB was a well-defined feature in the data.

Dynamic energy spectra and pitch-angle distributions of precipitating particles at the poleward edge of the auroral oval is well known to indicate the location of the OCB (Vampola, 1971). Here we use nightside auroral oval boundaries determined using the logical criteria of Newell et al. (1996) applied to energy spectra of precipitating particles measured on board the Defense Meteorology Satellite Program (DMSP) satellites. Using the Newell et al. nomenclature, the most equatorward of the electron (b1e) or ion boundaries (b1i) was taken as the equatorward boundary of the auroral oval, and the most poleward of the electron (b5e) or ion boundaries (b5i) was taken as the poleward boundary (i.e. the OCB). The boundary b4s is the "structured/unstructured boundary," considered here to be the boundary between the diffuse and discrete ovals. These auroral oval locations are superimposed as bold, vertical lines in subsequent range-time plots.

During the study days energy spectra were available from the four DMSP satellites, F12, F13, F14, and F15, during our study nights. Each satellite was in a Sun-synchronous, or fixed local time orbit. This meant there were only one or two auroral oval passes mapping to the radar field of view per night, including conjugate passes in the Northern Hemisphere. To extend the temporal coverage of boundary identifications, the Starkov (1994) statistical model of auroral oval boundaries was used to extrapolate the DMSP boundaries to the longitude of the radar measurements. However, the instantaneous auroral oval is unlikely to conform to any statistical model, especially during the expansion phase of substorms. To limit the magnitude of possible errors, the extrapolation was only applied to DMSP nightside boundaries identified within 2 hours of the beam 4 longitude (i.e. 147.2° ± 30°E). Note that for September 5 and October 31, the average and standard deviation of the magnitude of corrections applied to the DMSP poleward edges were 0.9° ± 1.0°Λ and 1.1° ± 1.0°Λ, respectively.

Three errors were involved in comparing DMSP and radar boundaries: (1) the error in mapping the DMSP measurements to magnetic latitude, probably <0.5°, (2) the error in mapping the radar scatter from group range to magnetic latitude, probably <1°, and (3) the error in extrapolating the DMSP boundaries to the longitude of the radar, probably <2°. Hence adding these errors in quadrature, $\sqrt{5.25°} \approx 2.3°$ is a rough estimate of the maximum, conceivable error when comparing the OCBs with the SWBs.

RESULTS

Figure 1 is a summary plot of the observations made during the evening of September 5, 2000. Part (a) shows Macquarie Island (MQI) fluxgate magnetometer *perturbations* in the geomagnetic *X* (North), *Y* (East), and *Z* (down) components. These were calculated by transforming the absolute values to corrected geomagnetic co-ordinates, and then subtracting the daily means to facilitate comparison with the radar measurements. MQI (54.5°S, 158.9°E; –65°Λ) is located just east of the TIGER field of view, and provides the most relevant measure of local auroral electrojet (*AE*) activity. Two small substorms occurred during this evening, with the ratio of *Z* to *X* perturbations indicating mostly westward current flow just poleward of MQI. The onset (O) of the first substorm occurred at 1402 UT, the peak expansion phase (P) at 1430 UT (~ –119 nT), and the recovery phase ended (R) at ~1633 UT. The onset of a second substorm occurred at 1659 UT, the peak expansion phase at 1813 UT (~ –103 nT), and the recovery phase ended at ~1938 UT.

Figure 1 (b) shows the range-time plot of spectral widths measured along TIGER beam 4. Three shades of grey are used to represent three different kinds of echoes. The light shade represents sea echoes identified by "FITACF" (Baker, 1995), the standard algorithm used by all SuperDARN radars to analyse the autocorrelation functions of received signals. The intermediate shade of grey represents ionospheric scatter with low spectral

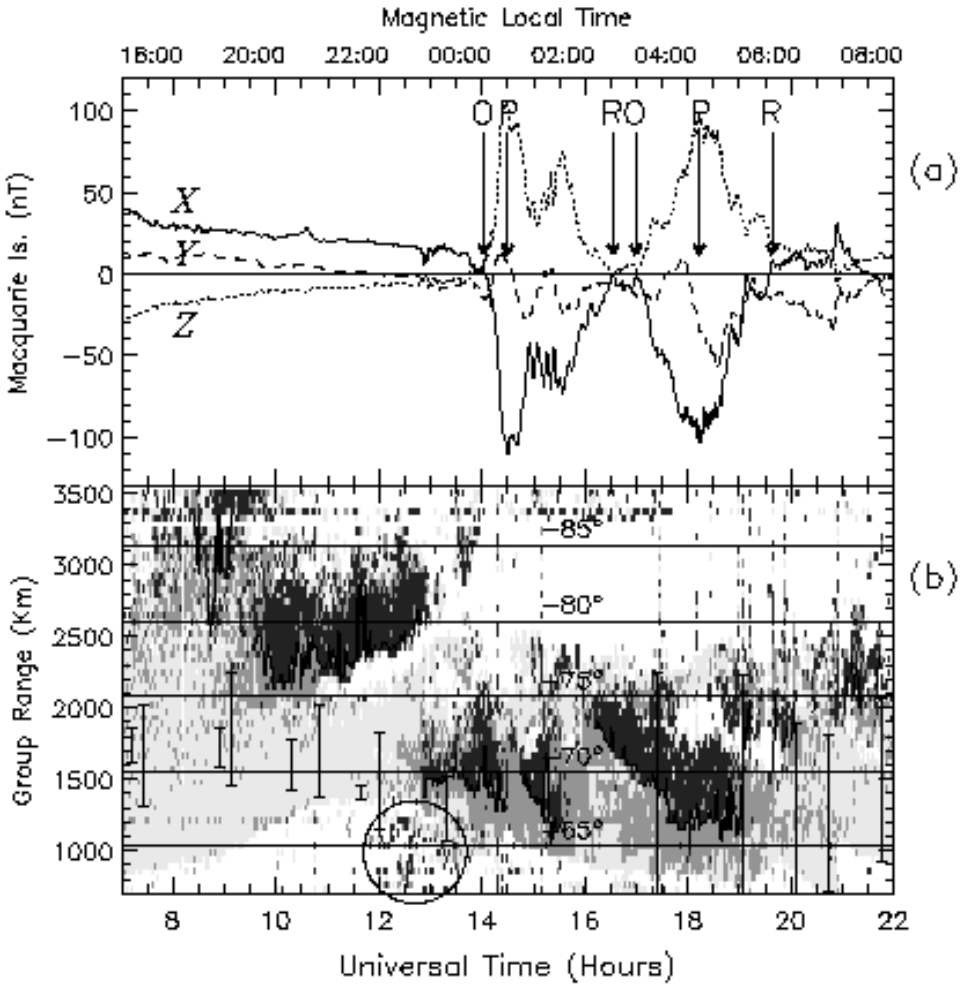

Fig. 1. (a) MQI magnetometer measurements of the geomagnetic *X* (solid), *Y* (dashed), and *Z* (dotted) perturbations at 1-min resolution during 07 to 22 UT on September 5, 2000. (b) Range-time plot of spectral widths measured along TIGER beam 4. This is "common mode" data recorded with 2-min resolution per beam. The thin horizontal lines represent magnetic latitudes between –65° and –85°, and MLT is shown at the top of the figure. Other details are described in the text.

widths <200 m s^{-1}, and the darkest shade represents ionospheric scatter with large spectral widths ≥200 m s^{-1}. As previously noted, the solid, fluctuating lines represent the automatically identified SWB, and the bold, vertical lines represent the corrected DMSP auroral oval locations. Horizontal bars are included to accentuate the locations of the equatorward and poleward edges, the latter indicating the OCB location.

Prior to ~1250 UT the SWB was not aligned with the OCB. The best agreement occurred for the F13 satellite pass at 1050 UT (within experimental error), near to when ionospheric scatter with low spectral width was located immediately equatorward of ionospheric scatter with large spectral width. The SWB was poorly defined prior to 0930 UT, and after ~1050 UT there was no ionospheric scatter with low spectral width immediately equatorward of the SWB. Moreover, the next two DMSP auroral oval locations were also superimposed upon first-hop seas echoes (light grey). This suggests that an unobserved SWB may have actually occurred where the radar was observing first-hop sea echoes. Hence the observed SWB may have been an artefact caused by leading edge, 1.5-hop rays entering the ionosphere in a region where large spectral widths extended much further equatorward. An examination of ionograms recorded at Hobart (–54°Λ) and MQI (–65°Λ) confirm that h_mF2, and hence the group delay to the apparent SWB, were increasing during ~1050 to 1250 UT.

Beyond 1250 UT there were more persistent ionospheric echoes with low spectral width immediately equatorward of the scatter with large spectral width. The OCB identified during the F15 satellite pass at 1320 UT agrees with the SWB. This identification occurred during the growth phase of the first substorm with onset at 1402 UT. The next two F13 satellite passes (1724, 1904 UT) were during the expansion and recovery phases, respectively, of the second substorm with onset at 1659 UT. The boundaries between the discrete and diffuse aurora were –66.4°Λ and –69.9°Λ, respectively, which agree much more closely with the SWB than the OCBs

located ~7° further poleward. During this substorm observed in the morning sector the SWB was a better proxy for the CPS/BPS boundary. The OCB identified during the remaining three F13 passes beyond 06 MLT (2006, 2045, 2147 UT) all agree with the patchy SWB within experimental error. No substorm occurred during this interval.

Figure 2 is a summary plot of the observations made during the evening of October 31, 2000. Part (b) shows the corresponding perturbations in the MQI geomagnetic *X*, *Y*, and *Z* components. Three substantial negative bays in the *X* component occurred during this evening. The onset (O) of a moderate substorm occurred at 1022 UT (~ –330 nT), the peak expansion phase (P) at 1047 UT, and the recovery phase ended (R) at ~1222 UT. The relatively small amplitude of the *Z* component suggests the westward electrojet was centred above MQI (–65°Λ). The onset of a lesser substorm occurred at 1443 UT (~ –118 nT), the peak expansion phase at 1513 UT, and the recovery phase ended at ~1601 UT. During this substorm the electrojet was located just poleward of MQI. Lastly, there was an impulsive increase in the *X* component at 1715 UT, immediately followed by an impulsive decrease, then a gradual increase. This sequence of events was initiated by the arrival of a dynamic pressure pulse in the solar wind. An analysis of this event is beyond the scope of this report.

Figure 2 (b) shows the range-time plot of spectral widths measured along TIGER beam 4, with annotations in the same format as Figure 1 (b). Prior to the onset of the first substorm at 1022 UT, there were small regions of large spectral width, but the SWB was poorly defined. Starting just prior to substorm onset and lasting until 1050 UT (just beyond peak expansion phase, 1047 UT), the radar measured ionospheric scatter with persistently large spectral widths >200 m s^{-1} extending equatorward to –64°Λ. Consequently, a well-defined SWB was identified during the expansion phase, in agreement with corrected DMSP OCBs identified by the F14 and F13 satellites (1033 and 1039 UT). The next four DMSP passes (1053, 1108, 1137, 1155 UT) were during the recovery phase ending near 1222 UT, and the poleward edges all agreed with the well-defined SWB within experimental error. Beyond the recovery phase the SWB fluctuated but trended equatorward, and the next three DMSP poleward edges (1251, 1320, 1339 UT) also agreed with the well-defined SWB.

A DMSP F13 pass occurred at 1711 UT, just prior to the arrival of the dynamic pressure pulse at 1715 UT, with a subsequent outage of radar backscatter due to enhanced absorption. A final F13 pass occurred at 1852 UT. In both cases the SWB was equatorward of the OCB. The boundary between discrete and diffuse aurora during these two passes were –72.4°Λ and –69.1°Λ, respectively, in reasonable agreement with the location of the observed SWB. However, the two OCBs were superimposed on 2^{nd}-hop sea echoes (light grey), so the HF propagation conditions did not favour the detection of a SWB located further poleward.

Full-scan data on September 05 (not shown) revealed an unusual population of intermittent ionospheric echoes with very large spectral widths (>600 ms^{-1}), much larger than the spectral widths normally residing poleward of the fluctuating SWB superimposed in part (b). Some of these echoes are apparent in part (b) during 12–14 UT (circled). They first appeared on the eastern-most beams at ~1030 UT, expanded westward through the field of view during the growth phase of the first substorm, and then disappeared on beam 10 during the expansion phase at ~1415 UT. They also occurred on closed field lines starting near the SWB at ~ –68°Λ, and extended equatorward to the limit of the radar field of view, –57°Λ. Their occurrence was sometimes concentrated into spatial regions 5° in longitude by 2° in latitude, and lasting for ~2–5 mins. Patchy ionospheric echoes, sometimes with large spectral widths, were also observed on closed field lines during various substorm phases on October 31 (circles).

DISCUSSION AND CONCLUSIONS

For the TIGER radar the SWB is most likely to mark the ionospheric footprint of a magnetospheric boundary when the radar scatter is obtained via 0.5-hop HF propagation. Furthermore, the scatter showing low and high spectral widths should be unambiguously located in the upper *E* or *F* region of the ionosphere, since different plasma instabilities operate in the lower *E* region. It is also important for the SWB identification to be based upon observations of persistent ionospheric scatter with a well defined transition from low to high spectral widths. The September 05 event illustrated these aspects well. Prior to ~1250 UT high spectral width scatter was observed but, because of HF propagation conditions, this was not bordered by low spectral width ionospheric scatter. The DMSP data shows the SWB did not mark a magnetospheric boundary on this occasion. After this time the scatter met our criteria and was associated with either the OCB or the CPS/BPS boundary. Clearly, changing propagation conditions are very important and partly explain why SuperDARN radars deployed at different locations tend to observe SWBs under various geophysical conditions.

The October 31 data in particular confirm the SWB was a reasonable proxy for the OCB in the pre-midnight sector during moderately disturbed geomagnetic conditions (Lester et al. 2001; Parkinson et al. 2002). This was shown by a sequence of 9 DMSP satellite passes, including 2 during substorm expansion, 4 during recovery phase,

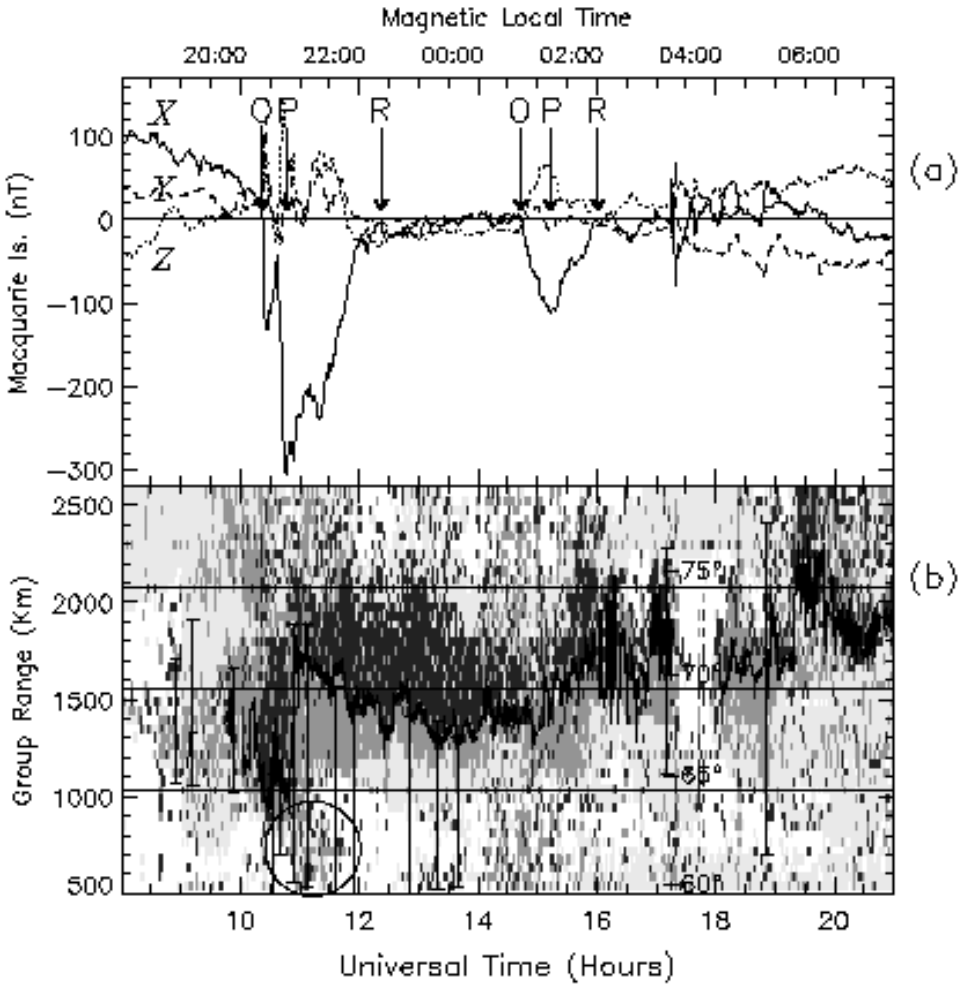

Fig. 2. (a) MQI magnetometer measurements of the geomagnetic *X* (solid), *Y* (dashed), and *Z* (dotted) perturbations at 1-min resolution during 08 to 21 UT on October 31, 2000. (b) Range-time plot of spectral widths measured along TIGER beam 4. This is discretionary mode data recorded with 6-s resolution along beam 4. The results are presented in the same format as Figure 1.

and 3 during a subsequent growth phase. Note that for the first substorms observed on both evenings, the OCB inferred from the SWB tended to contract poleward during the recovery phase. This suggests the effects of nightside reconnection did not prevail in our measurements until after the expansion phase. Without simultaneous measurements at many MLTs and modelling the effects of dayside and nightside reconnection rates, we cannot conclude whether our observations favour the near-Earth initiation model of substorm development (Lui, 2001).

The two DMSP passes during the expansion phase of the first substorm on October 31 show the SWB was a proxy for the OCB. However, this result is a tentative because extrapolating the DMSP boundaries to the MLT of the beam 4 may have large errors during expansion phase when the auroral oval develops complex longitudinal structure. It is also possible the geophysical processes responsible for the large spectral widths penetrate to closed field lines during unstable, substorm conditions. Enhanced ULF wave activity with Pc 1-2 periods in the range 0.1 to 10 s are a possible cause of the large spectral widths confined to the polar cap ionosphere (see André et al, 1999). Initial qualitative assessment of MQI induction magnetometer data recorded during our study nights suggests bursts of broadband ULF wave activity were coincident with times when large spectral widths were measured at –65ºΛ.

Observations made during both nights show the SWB changed from being a signature of the OCB before midnight to a signature of the CPS/BPS boundary in the morning sector (>03 MLT), irrespective of substorm phase. An absence of suitable DMSP passes during the early morning hours (~01–03 MLT) prevented us from determining whether there was a gradual or sudden change in the identity of the SWB beyond midnight. However we speculate the change occurred at ~1500 UT on October 31 when the occurrence of large spectral widths briefly diminished and contracted poleward. It is well known that auroral oval dynamics behave differently in the pre- and post-midnight sectors. For example, more energetic proton precipitation is observed further equatorward pre-midnight, and more energetic electron precipitation further equatorward post-midnight. Thus we wonder whether

changes in magnetospheric instabilities and corresponding ULF wave morphology undergo a transition after midnight.

The nightside SWB exhibits complex behaviour that we still do not fully understand. For example, the SWB is sometimes bifurcated in full-scan and range-time plots (i.e. not simply because structure in space and time is confused). This bifurcation may arise because the corresponding magnetospheric boundary is a porous surface, as opposed to the smooth surface normally imagined (Lui, 2001). Alternatively, the bifurcation might be caused by complex propagation conditions (e.g. spatial variations in ionospheric absorption and horizontal gradients in plasma density). Lastly, the possibility of multiple SWBs mapping to different magnetospheric boundaries must be considered. The tendency for spectral widths to sometimes decrease again toward the poleward edge of regions of large spectral widths provides for the possibility of another, unobserved SWB located further poleward. Hence there may be a preference for some SuperDARN radars to observe SWBs aligned with the OCB or CPS/BPS boundary, either simultaneously or at different MLTs, under different IMF and geomagnetic conditions.

An unusual population of intermittent ionospheric echoes with very large spectral widths (>600 m s^{-1}) was observed on closed field lines during the growth and expansion phase of the first substorm on September 05. The algorithm we used to automatically identify the SWB had sufficient spatial and temporal filtering to reliably discriminate the normal radar SWB amidst these echoes, thereby resulting in an accurate determination of the OCB during substorms. We presently do not understand the geophysical significance of these echoes, but there is a possibility they fore tell substorm onset.

The preceding assertions about the MLT and geomagnetic activity behaviour of the SWB are based upon two nights of observations. Clearly, they need more thorough testing using an extensive database of nightside SWB and DMSP OCB identifications sorted according to substorm phase. Nevertheless, we hope the present case studies provide further insights into when the HF radar SWB can be used as a reliable proxy for the OCB or CPS/BPS boundary, and also help in the development of automatic detection algorithms.

ACKNOWLEDGMENTS

This work was supported by the Australian Research Council and the Australian Antarctic Science Advisory Committee. The Australian Geological Survey Organisation is thanked for making available MQI fluxgate magnetometer data. P. Wilkinson of the IPS Radio and Space Services, Australia, is thanked for providing Hobart and MQI ionograms. P. Ponomarenko of the University of Newcastle, Australia, is thanked for providing dynamic spectrograms of MQI induction magnetometer data. The DMSP particle detectors were designed by D. Hardy of AFRL, and data obtained from JHU/APL. We thank D. Hardy, F. Rich, and P. Newell for its use. Finally, we thank the numerous people who contributed to the operation of TIGER.

REFERENCES

André, R., M. Pinnock, and A. S. Rodger, On the SuperDARN autocorrelation function observed in the ionospheric cusp, *Geophys. Res. Lett.*, **26**, 3353-3356, 1999.

Baker, K. B., Dudeney, J. R., Greenwald, R. A., et al., HF radar signatures of the cusp and low-latitude boundary layer, *J. Geophys. Res.*, **100**, 7671-7695, 1995.

Dudeney, J. R., A. S. Rodger, M. P. Freeman, J. Pickett, J. Scudder, G. Sofko, and M. Lester, The nightside ionospheric response to IMF By changes, *Geophys. Res. Lett.*, **25**, 2601-2604, 1998.

Greenwald, R. A., et. al., DARN/SuperDARN: A global view of the dynamics of high-latitude convection, Space *Sci. Rev.*, **71**, 761-796, 1995.

Lester, M., S. E. Milan, V. Besser, and R. Smith, A case study of HF radar spectra and 630.0 nm auroral emission in the pre-midnight sector, *Ann. Geophysicae*, **19**, 327-339, 2001.

Lui, A. T. Y., Current controversies in magnetospheric physics, *Reviews Geophys.*, **39**, 535-563, 2001.

Newell, P. T., Y. I. Feldstein, Y. I. Galperin, and C.-I. Meng, Morphology of nightside precipitation, *J. Geophys. Res.*, **101**, 10,737-10,748, 1996.

Parkinson, M. L., P. L. Dyson, M. Pinnock, et al., Signatures of the midnight open-closed magnetic field-line boundary during balanced dayside and nightside reconnection, *Ann. Geophysicae*, In Press, 2002.

Starkov, G. V., Mathematical model of the auroral boundaries, *Geomag. Aeronomy*, **34**, 331-336, 1994.

Vampola, A. L., Access of solar electrons to closed field lines, *J. Geophys. Res.*, **76**, 36-43, 1971.

E-mail address of M. L. Parkinson m.parkinson@latrobe.edu.au

Manuscript received 19 October 2002; revised ; accepted